ASTRONOMY & ASTROPHYSICS
SUPPLEMENT SERIES

Astron. Astrophys. Suppl. Ser. **145**, 405–414 (2000)

Box- and peanut-shaped bulges⋆,⋆⋆

I. Statistics

R. Lütticke, R.-J. Dettmar, and M. Pohlen

Astronomisches Institut, Ruhr-Universität Bochum, D-44780 Bochum, Germany
e-mail: luett@astro.ruhr-uni-bochum.de

Received May 11; accepted June 13, 2000

Abstract. We present a classification for bulges of a complete sample of ∼ 1350 edge-on disk galaxies derived from the RC3 (*Third Reference Catalogue of Bright Galaxies*, de Vaucouleurs et al. 1991). A visual classification of the bulges using the Digitized Sky Survey (DSS) in three types of b/p bulges or as an elliptical type is presented and supported by CCD images. NIR observations reveal that dust extinction does almost not influence the shape of bulges. There is no substantial difference between the shape of bulges in the optical and in the NIR. Our analysis reveals that 45% of all bulges are box- and peanut-shaped (b/p). The frequency of b/p bulges for all morphological types from S0 to Sd is > 40%. In particular, this is for the first time that such a large frequency of b/p bulges is reported for galaxies as late as Sd. The fraction of the observed b/p bulges is large enough to explain the b/p bulges by bars.

Key words: galaxies: evolution — galaxies: spiral — galaxies: statistics — galaxies: structure

1. Introduction

Several theories of bulge formation are currently discussed: primordial scenarios (monolithic collapse: Eggen et al. 1962 (ELS); clumpy collapse: Kauffmann et al. 1993, Baugh et al. 1996; inside-out formation: van den Bosch 1998; Kepner 1999), secular evolution scenarios (merger: Wyse et al. 1997 and references therein, dynamical evolution due to gravitational instabilities, such as bars: Combes et al. 1990), and combinations of both (Combes 2000). Therefore statistics of bulges are needed to test the proposed dynamical processes of bulge formation. Statistics of b/p bulges are of particular interest to demonstrate the importance of these structures for disk galaxies and to point out the relevant evolution scenarios of bulges in general. From the frequency of b/p bulges the likeliness of their formation process can be estimated.

External cylindrically symmetric torques (May et al. 1985) or mergers of two disk galaxies (Binney & Petrou 1985; Rowley 1988) as origins of b/p bulges require very special conditions (Bureau 1998). Therefore such evolutionary scenarios can explain only a very low frequency of b/p bulges. Accretion of satellite galaxies is a formation process of b/p bulges (Binney & Petrou 1985; Whitmore & Bell 1988), which could produce a higher frequency of b/p bulges. However, an oblique impact angle of the satellite is needed for the formation of a b/p bulge and a massive accretion event would disrupt the stellar disk (Barnes 1992; Hernquist 1993). The origin of b/p bulges by bars was first noticed by Combes & Sanders (1981). Combes et al. (1990) and Raha et al. (1991) substantially revived this idea. Comparisons between the frequency of barred galaxies and galaxies with a b/p bulge can test the probability of evolutionary scenarios of b/p bulges based on bars.

The estimated frequency of galaxies with a b/p bulge has steadily increased in former statistics from 1.2% (Jarvis 1986), over 13% (de Souza & dos Anjos 1987, hereafter SA87) and 20% (Shaw 1987), up to 45% (Dettmar & Barteldrees 1988). This rise results from differences in sample selection, sample size, detection method, and criteria to identify b/p bulges. However, the later three statistical studies have shown that b/p bulges are not really as peculiar as they were supposed to be in the past. Therefore very common processes are required to explain their high frequency. No complete statistics and list of galaxies with b/p bulges, based on observations, have been published in the last ten years. However,

⋆ Partly based on observations collected at ESO/La Silla (Chile), DSAZ/Calar Alto (Spain), and Lowell Observatory/Flagstaff (AZ/U.S.A.).

⋆⋆ Tables 6 and 7 are only available in electronic form at CDS via anonymous ftp to cdsarc.u-strasbg.fr (130.79.128.5) or via http://cdsweb.u-strasbg.fr/Abstract.html the knowledge about galactic evolution would greatly benefit from a reliable value for the frequency of b/p bulges by the determination of the most likely scenario for the formation of b/p bulges and subsequent conclusions on the evolution of bulges in general. A complete list of b/p bulges is a base for a detailed analysis of these structures.

In Sect. 2 we present our investigated sample of edge-on disk galaxies, and our classification of the bulge shape is explained in Sect. 3. The results of our statistics and of additional follow-up CCD observations in the optical and in the NIR are given in Sect. 4. Section 5 compares our findings to former statistics. In Sect. 6 we discuss our results and finally, in Sect. 7 we give the conclusions from our statistical analysis of the sample.

2. Sample selection

2.1. Former samples

The first search for b/p bulges was conducted by Jarvis (1986). By visual inspection of all fields of the ESO/SERC *J* sky survey he found therein 30 b/p bulges and listed additionally 11 galaxies with b/p bulges from the literature. Together with a control sample he estimated that about 1.2% of all disk galaxies possess b/p bulges.

Shaw (1987) inspected visually the ESO/SERC *J* and Palomar Observatory/National Geographical Survey (POSS) *B*- or *R*-band scanned survey plates. He derived a frequency of b/p bulges of 20(±4)% as a lower limit detecting 23 b/p bulges in a sample of 117 disk galaxies. The sample was mainly selected from the RC2 (*Second Reference Catalogue of Bright Galaxies*, de Vaucouleurs et al. 1976) and included disk galaxies with a diameter log $D_{25} \geq 1.55$ ($D_{25} \sim 3.5'$) at the 25 (B) mag arcsec^{-2} isophotal level and a "sufficiently" edge-on aspect.

Until today the largest investigated sample of 555 galaxies was presented by SA87. Their list was extracted from several catalogues and contained all disk galaxies with restricted total *B* magnitude ($B_{\rm T} < 13.2$ mag) and axis ratio ($b/a < 0.5$). The galaxies were inspected on film copies of the ESO Quick Blue survey or the POSS prints by means of a microscope. A "substantial number" of candidates were scanned using the PDS microdensitometer at ESO and checked with an image processing system (IHAP). In this way SA87 found 74 b/p galaxies as a lower limit. This is 13% of their total sample.

A much larger frequency of b/p bulges was proposed after the investigation of 73 galaxies obtained with CCD surface photometry (Dettmar & Barteldrees 1988; Dettmar 1989). That sample gave a frequency of 45(±8)% and Dettmar (1996) concluded from this sample a lower limit of the total frequency of b/p bulges of 35%. However, only 15 objects with b/p bulge from this sample were listed by name in a paper of Shaw et al. (1990) together with other known b/p bulges from the literature.

2.2. New sample selection

The former statistics in mind a new one should contain a large number of galaxies, be complete, and based on a detection method for the b/p bulges with reasonable accuracy. In the new statistics presented here the completeness with regard to the size of a galaxy is reached by the selection of all disk galaxies ($-3.5 < T < 9.5$) out of an electronic version of the RC3 with diameters larger than $2'$ ($\log D_{25} \geq 1.3$). For disk galaxies without known T parameter it is determined separately (see notes to Table 6). Extracting the sample from one catalogue is preferable to the method of SA87 since the parameters differ among the catalogues and an exact selection criterion is impossible. Similar to Shaw (1987) the selected sample is diameter limited, but compared to his sample the limit is nearly 2 times smaller. Additionally, the use of the newer catalogue (RC3 instead of RC2) leads to a much larger number of investigated galaxies. Restricting the sample in diameter and not in $B_{\rm T}$ magnitude is preferred because the RC3 attempts to be complete for galaxies with an apparent diameter larger than $1'$ at the D_{25} isophotal level and in addition, the $B_{\rm T}$ magnitude is not even listed for all galaxies larger than $2'$. Therefore a magnitude limit would not result in a complete sample. Furthermore, a magnitude limit would prefer the selection of early type galaxies.

Since b/p bulges can only be observed at inclinations down to $i \sim 75°$ (Shaw et al. 1990), in a first step all face-on galaxies are excluded using the axis ratio according to SA87. S0 galaxies ($-3.5 < T \leq -0.5$) with $\log R_{25} \geq 0.30$ and other disk galaxies with $\log R_{25} \geq 0.35$ are included ($R_{25} = \frac{a}{b}$). These different limits are used since the transformation of the axis ratio into the inclination angle depends on the morphological type (Bottinelli et al. 1983; Guthrie 1992). With different formulae (the simplest is $\cos i = \frac{b}{a}$; see references in Guthrie 1992) this restriction results for disk galaxies in a limit for the inclination angle i between 60° and 70° degree. This limit ensures most likely a detection of all observable b/p bulges. The final sample meeting these selection criteria contains 1343 galaxies.

The preferable method to classify a b/p bulge is the use of CCD images, but for the whole sample the amount of observing time would be unreasonably large. Therefore all galaxies are inspected using the Digitized Sky Survey (DSS)[1]. This survey is complete over the whole sky and an investigation of the images of the galaxies with data analysis software is possible. The DSS is based on photographic surveys of the northern POSS *E* plates (*R*-band, $m_{\rm lim} = 20.0$ mag), the southern SERC *J* plates (equivalent to *B*-band, $m_{\rm lim} = 23.0$ mag), and the southern Galactic plane SERC *V* plates (*V*-band, $m_{\rm lim} = 14.0$ mag) (McLean 1999) and has a scale of $1.7''$ pixel^{-1}. Galaxies which are saturated in their central regions are checked (if possible) with the ESO Lauberts-Valentijn Archive (Lauberts

[1] http://arch-http.hq.eso.org/cgi-bin/dss

& Valentijn 1989) kindly made available by ESO[2]. While the images within the ESO Lauberts-Valentijn Archive are not saturated and have a better scale (1.35″ pixel^{-1}), they have a lower signal-to-noise ratio compared to the images of the DSS.

3. Classification of box/peanut bulges

Shaw (1993a) and Lütticke (1996) derive objective parameters to characterize quantitatively b/p structures by the measurement of the excess luminosity and the total or maximal fraction of the b/p distortion (depending on the radial distance from the center) in relation to the observed bulge luminosity. However, the application of such a classification method is unpractical for a large sample of galaxies and strongly depends on the modelled luminosity distribution for the disk and the elliptical part of the bulge.

The a_4 isophote shape parameter is used by Combes et al. (1990), Shaw (1993a), Lütticke (1996), and Merrifield & Kuijken (1999) to quantify the degree of boxiness of bulges by measuring the deviations from perfect ellipses (e.g. Bender & Möllenhoff 1987). However, it is problematic that the determination of the extreme value of a_4 depends on the fitted region of the bulge. Fitting only the inner parts of bulges results in some galaxies in the undetection of the boxiness of the bulge which is most prominent in the outer parts. For instance the clear boxy bulge of NGC 1055 (Shaw 1993b; Lütticke et al. 2000b, hereafter Paper III) is undetected by Merrifield & Kuijken (1999) using the a_4 parameter. An additional disadvantage of the determination of this parameter is the influence of the masked stars in the foreground, dust, bars, and the extreme nature of b/p isophotal distortions for the ellipse fitting. Therefore the region of the galaxy which is used for the fitting is important. Shaw (1993a) uses the whole galaxy, Lütticke (1996) the disk subtracted galaxy, and Merrifield & Kuijken (1999) mask out a wedge-shaped region of each image within 12 degrees of the disk major axis and only fit "on the side of the galaxy where the disk projects behind the bulge".

These disadvantages lead to the fact that the a_4 parameter is not suitable for uniform classification of a large sample of bulges. Additionally, the resolution of the DSS images is too low to determine the a_4 parameter for the whole sample. Therefore the bulges of the investigated sample are classified by their degree of b/p shape derived by visual inspection from contour plots of the galaxy images.

Reshetnikov & Combes (1998) use similar arguments to choose a "straightforward procedure of eyeball estimation" with isophotal maps from the DSS instead of objective criteria for the detection and classification of warped disks.

[2] http://archive.eso.org/wdb/wdb/eso/esolv/form

The bulges are divided in three types of b/p bulges (**1** – **3**), elliptical bulges, and unclassifiable bulges.

- **1:** peanut-shaped bulge;
- **2:** box-shaped bulge;
- **3:** bulge is close to box-shaped, not elliptical;
- **4:** elliptical bulge;
- **5:** unclassifiable bulge.

Type **1** bulges are described by a depression along the minor axis on both sides of the main axis. In this way the bulge looks like a peanut (Fig. 1, top). The depth of the depression can be used as a characteristic parameter for these peanut-shaped bulges (Lütticke 1999). The box-shaped bulges (type **2**) are defined by isophotes parallel to the major axis. Therefore the bulge appears like a box (Fig. 1, second image). Some bulges of this class have a very prominent box form (Fig. 3, top). They could be type **1**, but due to low resolution of the images it is not possible to see the eventual depression along the minor axis. These bulges are called **2+**. The same class is used for bulges, which are on one side boxy and on the other peanut-shaped. Type **3** (Fig. 1, third image) is less well defined. These bulges possess a general flattening of the isophotes parallel to the major axis which is less pronounced as the flattening of type **2**. However, this flattening differentiates these bulges from the purely elliptical bulges of type **4** (Fig. 1, bottom). The limits between the classes are not sharp: obvious between **1** and **2**, clear between **2** and **3**, but sometimes indistinct between **3** and **4**. The classification of bulges can therefore in some cases be ambiguous, but a check of the whole sample (two independent classifications by the author and one of the co-authors) shows that more than 90% of the bulges are well defined by one of the different bulge types.

Several reasons are differentiated why bulges are not classifiable:

- **5.1:** Inclination is too far away from edge-on;
- **5.2:** Stars in the foreground projected onto the bulge;
- **5.3:** Galaxy is strongly perturbed;
- **5.4:** Dust conceals the shape of the bulge;
- **5.5:** Bulge is too small;
- **5.6:** Signal-to-noise ratio of the image is too low.

For galaxies which meet more than one of the above reasons only the most important one is listed (Tables 6 and 7). The classification for all galaxies in the sample with some minor changes after inspection of CCD images (Sect. 4.2) are given in Table 6.

4. Results

4.1. Statistics

About 3/4 of the Sdm and Sm galaxies are not at all classifiable and the rest is highly uncertain, because the bulges

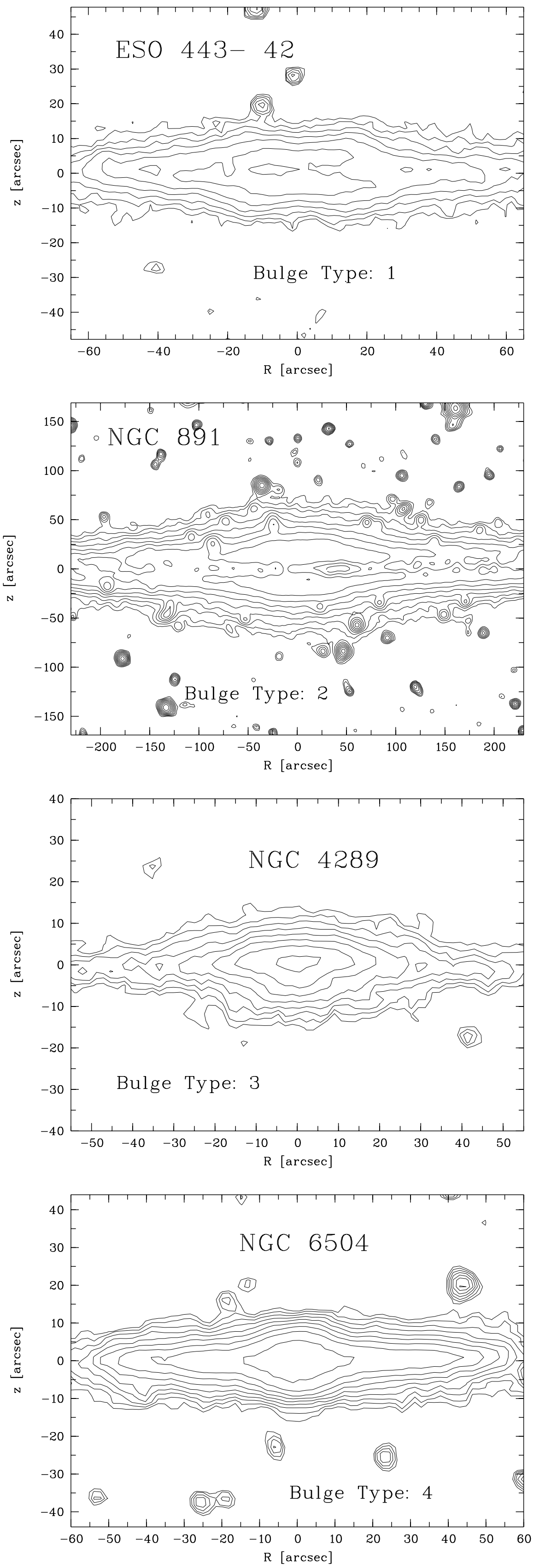

Fig. 1. Examples for the different bulge types from the DSS. Isophotes are logarithmically equidistant

of these galaxies — if they have any — are very small and faint and the influence of dust is very strong. Other structures like bars or star forming regions are more dominant. Therefore the selected sample is reduced to disk galaxies ranging from S0-Sd ($-3.5 < T < 7.5$) resulting in 1224 galaxies which will be investigated in the following.

40.0% of these bulges are unclassifiable, almost 3/4 of them due to an inclination which is too far from edge-on. This is an expected effect since the selection criterion of our sample for the inclination is a lower limit (see above). Only a few galaxies with a classifiable bulge in the sample have an axis ratio which is near to the sample limit of $\log R_{25} = 0.30$ (S0) and $\log R_{25} = 0.35$ (Sa − Sd), respectively. This shows that the limits are well chosen. There are only two peculiar edge-on galaxies known (with $\log D_{25} > 2'$) which have classifiable bulges and are not in our sample due to their low axis ratio (IC 2560 and NGC 7123). Therefore our list of galaxies with b/p bulges and a diameter larger than $2'$ is almost complete and the number of non-included b/p bulges is small.

Stars in the foreground (type 5.2) are responsible for 13% of unclassifiable bulges. These stars can influence the projected light from the galaxy in a way that the shape of the bulge cannot be identified. Dust lanes (5.4) prevent classifications in the same way, but only for a few galaxies, in which the dust lane has a large extension in comparison with the bulge size (see also Sect. 4.3). Their fraction decreases from late types and is equal to zero for galaxies earlier than Sbc. Scd and Sd galaxies have too small bulges (5.5) for classification, if their diameter is around the limit of $2'$ and their inclination is near to $90°$. At this orientation the measured diameter (D_{25}) and therefore the ratio of disk to bulge length is maximal due to optical depth effects (Xilouris et al. 1999). The result is that galaxies of the same morphological type and diameter (D_{25}) have bulges of different sizes which depend on the inclination angle. However, the fraction of galaxies in the sample having such small bulges is negligible (Table 1). In a few cases galaxies are in the southern Galactic plane (5.6), where the DSS has a higher surface brightness limit due to the use of the SERC V plates (see above). Therefore the images of the galaxies in this region have frequently a very small signal-to-noise ratio and the bulges appear to be too faint for classification. Perturbations (5.3) by interactions are only in a very few cases the reason for bulges being not classifiable.

Table 1. Reasons for the unclassifiability of bulges

bulge type	**5.1**	**5.2**	**5.3**	**5.4**	**5.5**	**5.6**
frequency	74%	13%	2%	4%	4%	3%

734 galaxies of our sample are classifiable (Table 2). From these galaxies we get a frequency of 45.0(±4.5)% b/p bulges (type **1** + **2** + **3**) (Table 2). The distribution

Table 2. Classifiable bulges binned by morphological type

	1	**2**[1]	**3**	**4**	Σ
S0/S0a	5	21	28	78	132
Sa/Sab	6	13	23	52	94
Sb/Sbc	14	44	65	136	259
Sc/Scd	5	28	53	100	186
Sd	0	9	16	38	63
Σ	30	115	185	404	734
%	4.1	15.7	25.2	55.0	100

[1]: 10.4% of all type **2** are **2+**.

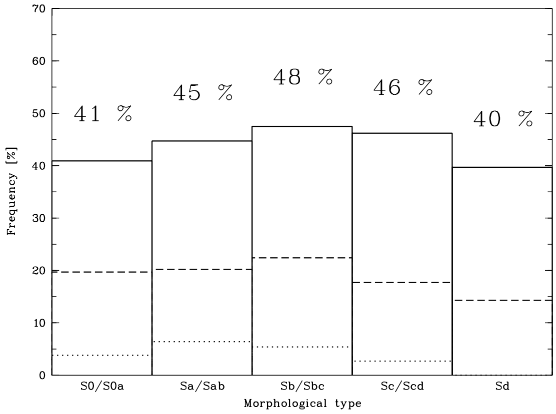

Fig. 2. Frequency of b/p bulges binned by morphological type derived from Table 2. Dotted lines: type **1**. Dashed lines: types **1** + **2**. Solid lines: all b/p types (**1** − **3**)

of all galaxies with b/p bulges binned by morphological type shows a weak maximum at Sb/Sbc galaxies (Fig. 2). The smallest fraction of b/p bulges is observed for early and late type disk galaxies. The fractions range from 40 to 48% in the maximum. From number statistics the errors are 4 − 7% for the frequencies of b/p bulges in each bin. Within these errors there is no dependence of the morphological type discernable. Regarding only galaxies with b/p types **1** and **2** the distribution is nearly the same. These results are in some aspects in contrast to the former investigations (see Sect. 5).

4.2. CCD observations

The optical CCD images were obtained in several observing runs between 1985 and 1998 at Lowell Observatory (1.06 m), Calar Alto (1.23 m), and ESO/ La Silla (0.9 m, 1.54 m, 2.2 m, and NTT). Standard reduction techniques for bias subtraction and flatfielding were applied. Individual short exposure frames of the galaxy were combined. The data are partly published in Barteldrees & Dettmar (1994), and Pohlen et al. (2000). Further data will be reported together with follow-up observations of b/p bulges in a separate paper (Lütticke et al. in prep.). In total we have observed 74 galaxies of our investigated RC3 sample up to now.

Only small differences (< 10%) between the classification of bulges comparing DSS (RC3 sample) and CCD images (Fig. 3 or Fig. 1 [top] and Fig. 4 [top]) are detected. Three bulges turned out to be type **4** rather than type **3** and two bulges are type **3** rather than type **4**. This could be explained by the higher resolution of the CCD images and the unsharp nature of the border between these two classes. However, the total frequency of b/p bulges is not changed. Bulges of type **2+** in the DSS images can be classified more accurately by the high resolution of the CCD images. If there is any depression along the minor axis (e.g. NGC 1886, Fig. 3), the bulge type is changed to **1**. If not, the bulge can be classified as (type **2**). Bulges which have only a depression along the minor axis on one side are still classified as type **2+**.

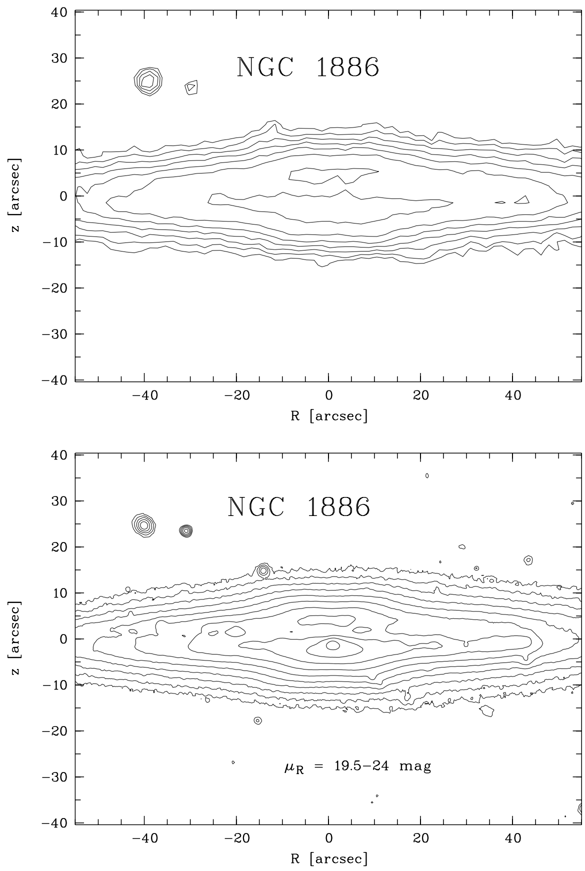

Fig. 3. Inspecting the DSS image (top) it is hard to decide, if there are depressions along the minor axis of NGC 1886 (first classified as bulge type **2+**) on both sides of the galaxy plane. The contour plots of the CCD images (NGC 1886: ESO/2.2 m, 30 min in r) reveal that NGC 1886 has a peanut bulge (bulge type **1**)

The comparison of the CCD with the DSS images shows that neither the low resolution, nor the saturated bright parts of some galaxies, nor the low signal-to-noise ratio, nor unresolved structures (small stars in the foreground) strongly influence the classification. Therefore the results of the statistics, which are derived from the RC3 sample and inspected with the DSS, are strongly supported by the CCD observations. Furthermore, the 33 galaxies observed in different optical filters reveal the same shape of the bulge. Therefore the classification of bulges at optical wavelengths is independent of the filter.

47 bulges of galaxies not included in the investigated RC3 sample (45 have $D_{25} < 2'$, additionally, one galaxy has $\log R_{25} < 0.35$, and one S0 galaxy has $\log R_{25} < 0.30$) are classified on CCD images of our observing runs (Table 7).

4.3. NIR observations

The essential advantage of investigations in the NIR is the small extinction by dust at these wavelengths (Knapen et al. 1991). Therefore the possible influence of the dust lane near the galactic plane in edge-on galaxies on the bulge shape is largely reduced by NIR observations. Our NIR sample of galaxies with classifiable bulges consists of 60 galaxies (Lütticke et al. 2000a, hereafter Paper II). It reveals that 75% of the bulges have the same bulge type in the optical as well as in the NIR (Table 3). 21% of the bulges are classified in the NIR to the next lower class, these bulges are less box-shaped. The change of the bulge type is for two bulges in the opposite way, one of them from a boxy to a peanut bulge likely due to the low resolution and saturation of the DSS image of this galaxy (NGC 5166).

Table 3. Differences in the classification of bulges in the optical and NIR

opt. bulge type	4	4	3	3	3	2	2	2	1	1
NIR bulge type	4	3	4	3	2	3	2	1	2	1
no. of galaxies	12	1	7	9	0	5	12	1	0	9

All peanut bulges prominent in the optical have the same shape in the NIR (e.g. ESO 443-42, Fig. 4). A detailed inspection of the galaxies having less boxy bulges in the NIR shows that dust is a possible explanation only for up to one third of these bulges. Differences in classification can be explained mainly by general uncertainties in the classification, the low resolution in the DSS — there is no difference between classifications derived from optical CCD and NIR images —, and low quality of some NIR images (bad seeing). The bulges whose classes are changed can frequently be marked as intermediate types (types **2** − **3** and **3** − **4**), respectively. Additionally, seeing conditions around 3″ weaken the boxy structure and over 50% of the bulges whose class changes were observed under such conditions.

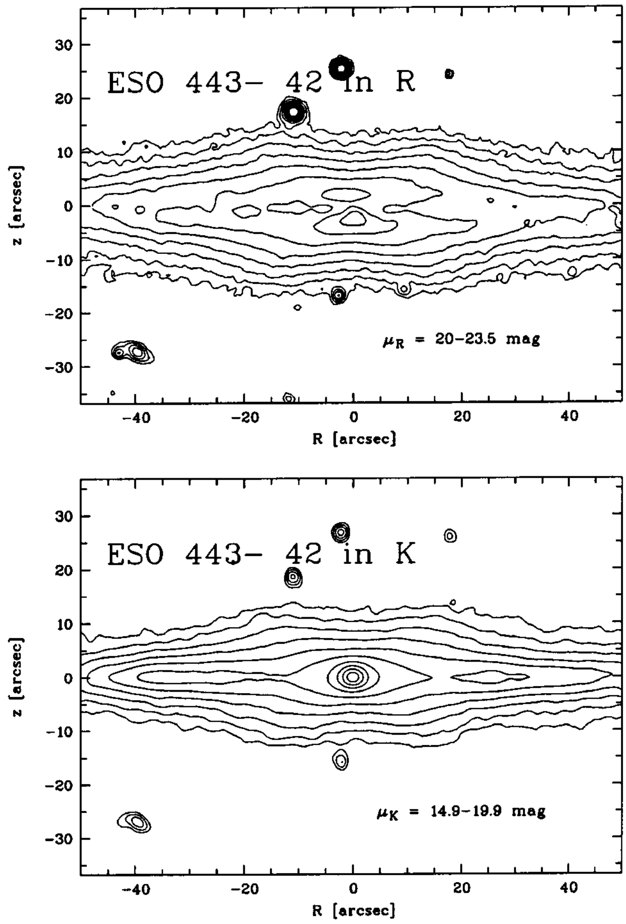

Fig. 4. The peanut bulge of ESO 443-42 is prominent in optical CCD images as well as in the NIR. Top: 0.9 m/ESO, 10 min in R. Bottom: 2.2 m/ESO, 23 min in K'

Images of galaxies observed in all three NIR filters J, H, and K reveal no difference in the bulge shape. Therefore the bulge classification seems to be same in a large region of wavelengths from the optical (350 nm) to the NIR (2.2 μm).

5. Comparison with former statistics

The low frequency of b/p bulges (1.2%) in the sample of Jarvis (1986) seems to result from the limitation to objects of very small diameters (Shaw 1987). Such a restriction, coupled with the used visual detection method on the plates of the ESO/SERC J sky survey, results in a non-detection of many b/p bulges and in the erroneously small frequency of b/p bulges. However, his division in box (**B**) and peanut-shaped (**P**) bulges is in agreement with our classification of b/p bulges. Considering only galaxies included in both samples, 3/4 of the galaxies of type **P** correspond to our bulge type **1** and type **B** to bulge type **2**, respectively. All galaxies with b/p bulges listed by Jarvis (1986) are also classified here as b/p bulges.

However, his statistics are based on a too small number of galaxies being representative. Additionally, his sample is biased with galaxies of known b/p bulge characteristics from the literature, therefore the conclusion with regard to a dependence of b/p bulges on the Hubble type is not meaningful.

Shaw (1987) uses a similar definition for his selection criterion of b/p bulges (depression along the minor axis or a general flattening of the isophotes) as we do, but without classification. The low frequency of 20%, he states, can be explained by the fact that galaxies with b/p bulges of type **3** are almost completely neglected. Counting only types **1** and **2** in our investigated sample results also in a frequency of 20% (Table 2). However, some prominent b/p bulges are missed by excluding peculiar disk galaxies (e.g. NGC 3628), galaxies which are far from edge-on (e.g. NGC 7582: Quillen et al. 1997), or by simply ignoring others (e.g. NGC 2424: Pohlen et al. 2000). On the other side there are two galaxies (NGC 1596 and NGC 4958) in his list of b/p bulges which have obviously an elliptical bulge. The sample also shows a maximum in the distribution of galaxies with b/p bulges concerning the morphological type of these galaxies at Sb/Sbc galaxies (Table 5). However, the frequencies in the individual bins are much smaller reflecting the total low frequency of b/p bulges. Additionally, the lack of Sd galaxies and the small frequency of Sc/Scd galaxies with b/p bulges are remarkable. That is in contrast to the rather high percentage of late type galaxies with b/p bulges which we have found in our study. The low frequency of Sc/Scd galaxies and the lack of Sd galaxies with b/p bulges are likely a result of the faint nature of bulges and therefore also of their b/p structures. Our method of detection using the DSS and new data analysis systems could explain the differences to Shaw (1987) in the bins of the late types, although both investigations are based on the same photographic material.

SA87 define three classes of galaxies marked by the degree of separation between disk and bulge, and by the form of the bulge. Additional to the mixture of these two criteria, it must be mentioned that their class III is defined as "cigar shaped" bulge. Therefore this class has nothing in common with b/p bulges. This reveals their prototype for class III (NGC 1380) and the high fraction of elliptical bulges (68%) in the class III sample (Table 4). Therefore the title of their list "box-shaped galaxies" is misleading. However, it should be clear by their definition of the classes that they do not present a list and classification of b/p bulges. This was and is still misunderstood in the literature (e.g. Bureau & Freeman 1999). Therefore a strong correlation between their types and our new introduced bulge types of the galaxies in both samples cannot be expected and is indeed not present (Table 4). However, their types I and I-II ("clear rectangular or peanut shape") should be classified also in our system as b/p bulge, but four galaxies (∼ 25%) out of these types have clear elliptical bulges (e.g. NGC 6504, Fig. 1, bottom). They also missed, likely due to the bad resolution of the images, some bright galaxies with prominent b/p bulges (e.g. NGC 3079: Shaw et al. 1993; Veilleux et al. 1999; NGC 7582: Quillen et al. 1997). Therefore their list is far from being complete and the frequency of b/p galaxies derived by SA87 is not comparable to the frequency of b/p bulges derived in our investigation. The statistics with regard to the Hubble type are not comparable due to the different definition of b/p bulges. In this way it is not surprising that the maximum in the distribution of b/p galaxies is reached for S0 galaxies and clearly lower values for intermediate types (Sa/Sb) in SA87 (Table 5) are not detectable in our distribution of b/p bulges.

Table 4. Our classification compared to SA87's classification

		bulge type			
		1	**2**	**3**	**4**
galaxy class from SA87	I	6	2	4	4
	II	4	9	8	12
	III	0	2	4	13

Listed are the numbers of galaxies.

Our derived frequency of b/p bulges is in excellent agreement with the result of Dettmar & Barteldrees (1988) and Dettmar (1989) who find a frequency of 45(±8)%. Their detection method by use of CCD images seems to prevent a misclassification. All five galaxies in their sample of b/p bulges (published in Shaw et al. 1990) and our sample have bulge types **1** or **2**. Dettmar's (1989, 1996) statistics concerning the Hubble type reveal also a maximum in the distribution of galaxies with b/p bulges at Sb/Sbc galaxies. However, the differences between the individual bins are much larger than in our statistics (Table 5). This can be explained by statistical errors due to the small sample size of 73 galaxies. Dettmar (1989, 1996) has also not found any Sd galaxy with b/p bulge in contrast to the frequency of 40% Sd galaxies with b/p bulges in our study. However, the lack of Sd galaxies is likely a result of the small number of investigated Sd galaxies in his sample. Additionally, the already mentioned faint nature of bulges of late type galaxies and the uncertainties in the classification of bulges increasing to later types (see above) lead to the fact that the boxiness of late type bulges could be missed. Even in small samples, where the possibility of comparison between the different forms of Sd bulges is not given, the detection of b/p bulges could be influenced. No detection of a type **1** b/p bulge in galaxies later than Sc in our sample could have similar reasons, if bulge type **1** in late type galaxies exists at all.

Galaxies in previously studied samples, which do not fulfill the selection criterion of our investigated sample due to morphological misclassifications of the Hubble type or too small diameters or axis ratios, are listed in Table 7. However, most of these galaxies have $D_{25} < 2'$ and therefore their classification with the DSS and ESO Lauberts-Valentijn Archive is uncertain.

Table 5. Comparison of different statistics: frequencies of b/p bulges according to their morphological type

	S0/S0a	Sa/Sab	Sb/Sbc	Sc/Scd	Sd
SA87	33%	13%	15%	3%	–[1]
Shaw[2]	25%	33%	36%	8%	0%
Dettmar[3]	46%	29%	61%	42%	0%
this study	41%	45%	48%	46%	40%

[1]: no Sd galaxy in sample; [2]: frequencies derived from Table 2 of Shaw 1987; [3]: frequencies derived from Fig. 1 of Dettmar 1989).

6. Discussion

The new classification of bulges is very similar to the types used by Jarvis (1986) and Shaw (1987). The frequency of 45% b/p bulges is consistent with Dettmar & Barteldrees (1988), Dettmar (1989) and the frequency of 20% prominent b/p bulges with Shaw (1987). However, the derived frequency is now based on a much larger sample of 734 galaxies. Furthermore, for the first time a large fraction of b/p bulges in galaxies as late as Sd is found, and some previously unknown peanut bulges (type 1) are listed (Tables 6 and 7).

The large fraction of b/p bulges (45%) shows that such bulges are not that peculiar but rather quite normal. Therefore very common processes are required to explain the origin of b/p bulges.

In order to check possible formation processes relating b/p bulges with bars, we have compared the frequency distributions of galaxies with b/p bulges and barred galaxies. The frequency distribution of barred galaxies is derived from RC3 (only face-on galaxies) and contains 8587 galaxies (Fig. 5). Both distributions binned by morphological type show the same general dependence. The maximum for barred galaxies is also at Sb/Sbc and the minimum at S0/S0a galaxies. This minimum is more distinct for barred galaxies as for galaxies with b/p bulge. However, for all galaxies the fraction of barred galaxies is 55% (nearly 2/3 of them are strongly barred [SB] and the rest weakly barred [SAB = SX]) in relation to 45% of galaxies with b/p bulges. This high percentage of barred galaxies is also recently confirmed by Knapen et al. (2000). Furthermore, it is remarkable that the percentage of barred Sd galaxies is relatively high compared to the minimal frequency of galaxies with b/p bulges for Sd galaxies. However, it should be mentioned that our error of this bin is the largest due to low number statistics (Table 2). Other statistics of barred galaxies taken from older catalogues (Sellwood & Wilkinson 1993) show the same general dependences, although the percentages vary mainly due to different fractions of weakly barred galaxies in the catalogues. However, former samples contain a much smaller number of galaxies (Sellwood & Wilkinson 1993). Unfortunately, the galaxies are not all classified as SB, SX, or SA (unbarred galaxy), but there is also a group of galaxies without any classification (S. = 28%). These galaxies can be likely interpreted as unbarred galaxies (as done in Fig. 5), because in former times unbarred galaxies were simply called "S", but they add uncertainties to the quantitative conclusion.

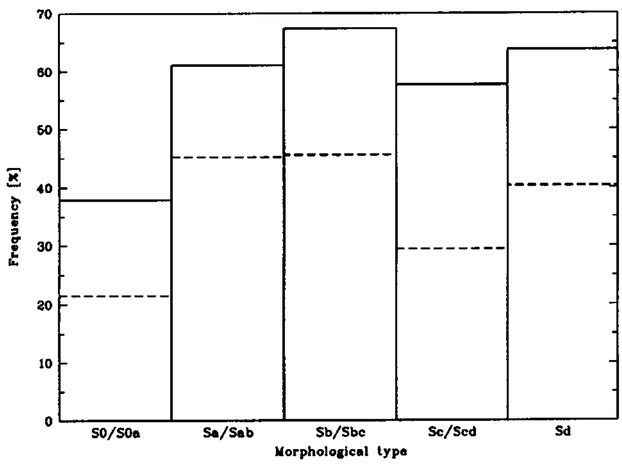

Fig. 5. Frequency of barred galaxies binned by morphological type. All face-on galaxies of the RC3 are included, i.e., all galaxies with a diameter (D_{25}) larger than $1'$ and an axis ratio smaller than 1/3 ($\log R_{25} < 0.477$). Solid lines: strongly barred (SB) plus weakly barred (SX) galaxies. Dashed lines: only SB galaxies

Bars as origin for b/p bulges (Combes et al. 1990; Raha et al. 1991; Pfenniger & Friedli 1991) are supported by the similarity in frequency distributions of galaxies with b/p bulges and barred galaxies. The fraction of b/p bulges is large enough to explain the b/p bulges by bars. The higher frequency of barred galaxies can easily be explained by the aspect angle of bars. End-on bars result for edge-on galaxies in elliptical shaped bulges, bars with intermediate aspect angles in boxy bulges, and edge-on bars in peanut bulges (Combes et al. 1990; Pfenniger & Friedli 1991, Paper II). Therefore our statistical results are consistent with recent studies stating a strong correlation of bars and b/p bulges. Bureau & Freeman (1999) and Merrifield & Kuijken (1999) find in observations of gas kinematics the characteristic "figure-of-eight" rotation curve, which is a strong signature for the presence of a bar, in many galaxies with b/p bulges. Direct kinematic evidence for streaming motions of a bar in two galaxies with a b/p bulge are reported by Veilleux et al. (1999). Kinematical bar diagnostics in edge-on spiral galaxies using simulations

Table 6. List of galaxies in the RC3-sample with bulge classification

(1) Object	(2) RA (2000)	(3) DEC (2000)	(4) bulge type	(5) NIR bulge type	(6) earlier detections	(7) T	(8) log D_{25}	(9) log R_{25}
IC 5376	00 01	+34 31	4			2.0	1.30	0.76
NGC 7814	00 03	+16 08	4^f			2.0	1.74	0.38
NGC 7817	00 03	+20 45	5.1			4.0	1.55	0.58
ESO 293- 34	00 06	−41 29	5.4			6.1	1.50	0.51
....	.. ..	.. ..	.	.	...	...	...	...
....	.. ..	.. ..	.	.	...	...	...	...
IC 2531	09 59	−29 36	1^c		J P, SA I, S	5.3	1.84	1.09
NGC 3079	10 01	+55 40	1		S	5.0^3	1.90	0.74
NGC 3098	10 02	+24 42	3^f	3	SA I	−2.0	1.36	0.57
....	.. ..	.. ..	.	.	...	...	...	...
....	.. ..	.. ..	.	.	...	...	...	...

The complete Table 6 with its notes and Table 7 are published in electronic form at CDS.

of families of periodic orbits and hydrodynamical simulations confirm the connection between bars and b/p bulges (Bureau & Athanassoula 1999; Athanassoula & Bureau 1999). Additionally, we find in our NIR study (Paper II) a strong correlation of bar signatures with b/p bulges. However, by finding a few bulges with a very complex morphology, we do not exclude that some b/p bulges result from a recent merger event (Dettmar & Lütticke 1999, Paper III).

The optical CCD images verify our classification of bulges and thereby the statistics derived by the DSS images. For the analysis of faint structures and more objective parameters of b/p bulges (e.g. parameter for the depression at the minor axis) CCD images are necessary. The best parameter for an objective classification of bulges would be the minimum of the a_4 parameter determined in the NIR (minimizing the dust influence) and after subtraction of a modelled disk and bar. However, models of high quality need images with a high signal-to-noise ratio. This would result in unreasonably observing time for the whole RC3 sample. Therefore the classification by visual inspection seems to be the best method until CCD data of the whole sky are available (e.g. for the northern sky: Sloan Digital Sky Survey).

Furthermore, it is shown by NIR observations that dust is not an important factor for the classification of b/p bulges. Therefore they are indeed present in disks of late type spirals as pointed out previously by Dettmar & Ferrara (1996). This result is not in contrast to Baggett & MacKenty (1996) who verify b/p structures in the NIR only in four out of six galaxies because their sample contains several misclassifications from older literature lists (Sects. 2.1 and 5). The comparison of optical and NIR images of b/p bulges reveals that there is no difference between the shape of bulges in different wavelengths bands or the differences are smaller than the uncertainties of the classification.

Additionally, as a byproduct a new catalogue of edge-on galaxies with $D_{25} > 2'$ confirmed by visual inspection is formed by our classification of bulges. This method gives a homogeneous sample of highly inclined galaxies compared to samples selected only by axis ratio and morphological type. This catalogue includes all galaxies with a bulge of types $1-4$ and $5.2-5.5$ (Table 6).

7. Conclusion

The bulge shape of a large sample of edge-on galaxies was investigated using DSS, CCD images in the optical wavelengths regime and in the NIR. Our main conclusions are:

- We have presented a visual classification of bulges in three b/p types and one elliptical type;
- 45% of all disk galaxies (S0 − Sd) have a b/p bulge. This fraction is based on a sample of 734 galaxies;
- For the first time a large fraction (40%) of b/p bulges in Sd galaxies is found;
- Comparisons between the fraction of barred galaxies and galaxies with b/p bulges show that b/p bulges can be explained by evolution scenarios based on bars;
- NIR observations reveal that dust is not responsible for the shape of b/p bulges;
- The shape of bulges is constant over a large region of wavelengths (350 nm − 2.2 μm).

Acknowledgements. Part of this work was supported by the *Deutsche Forschungsgemeinschaft, DFG*. This research has made use of the NASA/IPAC Extragalactic Database (NED) which is operated by the Jet Propulsion Laboratory, California Institute of Technology, under contract with the National Aeronautics and Space Administration. It also uses the Digitized Sky Survey (DSS) based on photographic data obtained using Oschin Schmidt Telescope on Palomar Mountain and The UK Schmidt Telescope and produced at the Space Telescope Science Institute.

References

Athanassoula E., Bureau M., 1999, ApJ 522, 699

Baggett S.M., MacKenty J.W., 1996, Box/Peanut Galaxies in the Near-IR, in: Buta R., Crocker D.A., Elmegreen B.G. (eds.), ASP Conf. Ser. 91, Barred Galaxies, p. 224

Barnes J.E., 1992, ApJ 331, 699

Barteldrees A., Dettmar R.-J., 1994, A&AS 103, 475

Baugh C.M., Cole S., Frenk C.S., 1996, MNRAS 283, 1361

Bender R., Möllenhoff C., 1987, A&A 177, 71

Binggeli B., Sandage A., Tammann G.A., 1985, AJ 90, 1681, VCC

Binney J., Petrou M., 1985, MNRAS 214, 449

Bottinelli L., Gouguenheim L., Paturel G., de Vaucouleurs G., 1983, A&A 118, 4

Bureau M., 1998, Bars in Edge-On Spiral Galaxies, Ph.D. Thesis. The Australian National University

Bureau M., Athanassoula E., 1999, ApJ 522, 686

Bureau M, Freeman K.C., 1999, AJ 118, 126

Combes F., 2000, Bulge Formation, in: Hammer F., Thuan T.X., Cayatte V., Guiderdoni B., Tran Thanh Van J. (eds.), Building Galaxies: from the Primordial Universe to the Present, Proceedings of Rencontres de Moriond. Ed. Frontières, p. 413

Combes F., Sanders R.H., 1981, A&A 96, 164

Combes F., Debbasch F., Friedli D., Pfenniger D., 1990, A&A 233, 82

de Souza R.E., dos Anjos S., 1987, A&AS 70, 465 (**SA87**)

Dettmar R.-J., 1989, Box- and Peanut-Shaped Bulges of Disk Galaxies, in: Corwin H.G., Bottinelli L. (eds.). The World of Galaxies. Springer, p. 229

Dettmar R.-J., 1996, Galactic bulges as an evolutionary phenomenon, in: Blitz L., Teuben P. (eds.). IAU Symp. 169, Unsolved Problems of the Milky Way. Kluwer, p. 335

Dettmar R.-J., Barteldrees A., 1988, BAAS 20, 1085

Dettmar R.-J., Ferrara A., 1996, NIR imaging of the box/peanut bulge in NGC 4302, in: Bender R., Davis R. (eds.), IAU Symp. 171, New Light on Galaxy Evolution. Kluwer, p. 362

Dettmar R.-J., Lütticke R., 1999, Do some bulges result from merging? In: Gibson B.K., Axelrod T.S., Putman M.E. (eds.), ASP Conf. Ser. 165, The Third Stromolo Symposium: The Galactic Halo, p. 95

de Vaucouleurs G., de Vaucouleurs A., Corwin Jr. H.G., 1976, Second Reference Catalogue of Bright Galaxies (RC2). University of Texas Press

de Vaucouleurs G., de Vaucouleurs A., Corwin Jr. H.G., Buta R.J., Fouqué P., 1991, Third Reference Catalogue of Bright Galaxies (RC3). Springer

Eggen O., Lynden-Bell D., Sandage A., 1962, ApJ 136, 748

Guthrie B.N.G., 1992, A&AS 93, 255

Haynes M.P., Herter T., Barton S., Benensohn S., 1990, AJ 99, 1740

Hernquist L., 1993, ApJ 409, 548

Jarvis B.J., 1986, AJ 91, 65

Kauffmann G., White S.D.M., Guiderdoni B., 1993, MNRAS 264, 201

Kepner J.V., 1999, ApJ 520, 59

Knapen J.H., Hes R., Beckman J.E., Peletier R.F., 1991, A&A 241, 42

Knapen J.H., Shlosman I., Peletier R.F., 2000, ApJ (in press)

Kraan-Korteweg R.C., 1982, A&AS 47, 505

Lauberts A., 1982, The ESO/Uppsala Survey of the ESO-B Atlas, ESO

Lauberts A., Valentijn E.A., 1989, The Surface Photometry Catalogue of the ESO-Uppsala Galaxies, ESO

Lütticke R., 1996, Flächenphotometrische Untersuchungen zu Eigenschaften von "box/peanut"-bulges in "edge-on" Scheibengalaxien, Diploma Thesis, Ruhr-Universität Bochum

Lütticke R., 1999, Box- and Peanut-Shaped Bulges, Ph.D. Thesis, Ruhr-Universität Bochum

Lütticke R., Dettmar R.-J., Pohlen M., 2000a, A&A (submitted) (Paper II)

Lütticke R., Dettmar R.-J., Pohlen M., 2000b, A&A (in preparation) (Paper III)

May A., van Albada T.S., Norman C.A., 1985, MNRAS 214, 131

McLean B., 1999, http://www-gsss.stsci.edu/dss/surveys.html

Merrifield M., Kuijken K., 1999, A&A 345, L47

Pfenniger D., Friedli D., 1991, A&A 252, 75

Pohlen M., Dettmar R.-J., Lütticke R., Schwarzkopf U., 2000, A&AS (in press)

Quillen A.C., Kuchinski L.E., Frogel J.A., Depoy D.L., 1997, ApJ 481, 179

Raha N., Sellwood J.A., James R.A., Kahn F.D., 1991, Nat 352, 411

Reshetnikov V., Combes F., 1998, A&A 337, 9

Rowley G., 1988, ApJ 331, 124

Sellwood J.A., Wilkinson A., 1993, Reports Progr. Phys. 56, 173

Shaw M.A., 1987, MNRAS 229, 691

Shaw M.A., 1993a, MNRAS 261, 718

Shaw M.A., 1993b, A&A 280, 33

Shaw M.A., Dettmar R.J., Barteldrees A., 1990, A&A 240, 36

Shaw M.A., Wilkinson A., Carter D., 1993, A&A 268, 511

Skiff B., 1999 (private communication)

van den Bosch F.C., 1998, ApJ 507, 601

Veilleux S., Bland-Hawthorn J., Cecil G., 1999, AJ 118, 2108

Whitmore B.C., Bell M., 1988, ApJ 324, 741

Wyse R.F.G., Gilmore G., Franx M., 1997, ARA&A 35, 637

Xilouris E.M., Byun Y.I., Kylafis N.D., Paleologou E.V., Papamastorakis J., 1999, A&A 344, 868

Yasuda N., Okamura S., Fukugita M., 1995, ApJS 96, 359

Yasuda N., Fukugita M., Okamura S., 1997, ApJS 108, 417